

## Structures and Organization of Bacteriochlorophyll c's in Chlorosomes from a New Thermophilic Bacterium *Chlorobium tepidum*

Tsunenori NOZAWA,\* Katsunori OHTOMO, Manabu SUZUKI, Yumi MORISHITA, and Michael T. MADIGAN†  
Department of Biochemistry and Engineering, Faculty of Engineering, Tohoku University, Aoba, Aramaki, Aoba-ku, Sendai 980

† Department of Microbiology, Southern Illinois University at Carbondale, Carbondale, Illinois 62901-6508, U.S.A.

(Received July 17, 1992)

A new thermophilic bacterium *Chlorobium tepidum* contains two major bacteriochlorophyll c components whose periphery substituents at 4-position are either an ethyl or a propyl group. Both components possess ethyl groups at 5-position, and the ester alkyl groups at 7-position are farnesyl groups. As an aggregate structure in CDCl<sub>3</sub> a piggy-back type dimer was suggested on the basis of variations of <sup>1</sup>H NMR chemical shifts accompanied with the aggregate formation and of values of calculated ring current shifts. Bacteriochlorophyll c (BChl c) aggregates with absorption maxima around 677, 705, and 740 nm showed stepwise interchanges in hexane-dichloromethane with variations in BChl c concentrations and in solvent compositions. Exciton theoretical analysis of the stepwise spectral shifts predicted high ordered organization of BChl c, implying a model for rod-elements in chlorosomes.

Recently a new thermophilic photosynthetic bacterium named *Chlorobium (C.) tepidum* has been isolated.<sup>1)</sup> This is a family of *Chlorobiaceae*, a green sulfur photosynthetic bacterium. Green bacteria are characterized by a special light harvesting organ called a chlorosome which does not exist in purple photosynthetic bacteria.<sup>2,3)</sup> Electron microscopy observation showed that rod-like structures or "rod-elements" are present in chlorosomes and are parallel to the long-axis of chlorosomes.<sup>3)</sup> Chlorosomes are composed of pigments (bacteriochlorophyll (BChl) c's or d's), lipid, and proteins. Recently many observations showed that rod-elements themselves do not contain proteins as basic elements.<sup>4,5)</sup> BChl c aggregates formed in nonpolar solvents showed many physicochemical properties characteristic to native chlorosomes,<sup>6,7)</sup> which indicates that direct interactions among pigments play fundamental roles in organization of the rod-elements in chlorosomes. Several basic structural models have been presented thus far,<sup>7–10)</sup> however, organization of BChl c aggregates in the rod-elements are still open to investigations. BChl c of chlorosomes isolated from *C. tepidum* has an absorption maximum at 740 nm, which is greatly red-shifted from 668 nm of BChl c in polar organic solvents. The red-shifted absorption maximum is characteristic of aggregated BChl c in nonpolar solvents. Thus aggregation properties of BChl c are fundamental for elucidation of structures and functions of native chlorosome.

We have analyzed the pigment composition and identified structures of the major components of BChl c's in chlorosomes from the thermophilic green sulfur bacterium *C. tepidum*. Dimer structures of BChl c in CDCl<sub>3</sub> have been elucidated by values of ring current shift in <sup>1</sup>H NMR. Furthermore we have taken special attention on the findings of stepwise spectral changes of BChl c in hexane-dichloromethane, analyzed the phenomena by the exciton theory,<sup>11,12)</sup> and have addressed to high ordered organizations of BChl c aggregates.

### Experimental

**Materials and Methods.** *C. tepidum* was grown and its chlorosomes were isolated by using methods similar to those previously reported.<sup>1,13)</sup> BChl c was extracted with methanol (or chloroform) and purified as previously described.<sup>13,14)</sup> HPLC (Toso Bio-LC system) with ODS (TSK<sub>gel</sub> ODS-80T<sub>M</sub>) column was used for fractionation to the components. The elution solvent was composed of methanol and water with a volume ratio of 96:4. <sup>1</sup>H NMR spectra were recorded on a Bruker MSL400 FT NMR spectrometer equipped with a dual probe for <sup>1</sup>H and <sup>13</sup>C. Chemical shifts were referred to TMS. Purified BChl c was dissolved in CDCl<sub>3</sub> treated with Na<sub>2</sub>CO<sub>3</sub>.<sup>6)</sup> BChl c aggregates were formed in hexane-dichloromethane by adding dichloromethane solution of BChl c into a specific amount of hexane solution.<sup>6)</sup> Dichloromethane was treated with Na<sub>2</sub>CO<sub>3</sub> just before use. Calculations based on exciton theory were performed on an NEC microcomputer with a home-made program.

### Results and Discussions

Figure 1 shows an elution profile of the pigment solution after extraction from freeze-dried cells and purification by hexane precipitation. Two major components exist with numerous minor components. The two major fractions (called HPLC1 and HPLC2 in this paper), and two relatively larger peaks (designated by ① and ②) showed absorption spectra which are characteristic of BChl c in methanol solution (Fig. 2 for HPLC1 and data not shown for HPLC2, fractions ① and ②). Thus all four fractions have absorption maxima at 668.5 and 435.0 (±0.5) nm. These absorption peaks indicate that all four fractions contain the BChl c conjugate units. Many other minor components also showed similar absorption maxima. Therefore it revealed that the chlorosomes from the thermophilic green sulfur bacterium *C. tepidum* have two major BChl c components with many minor ones.

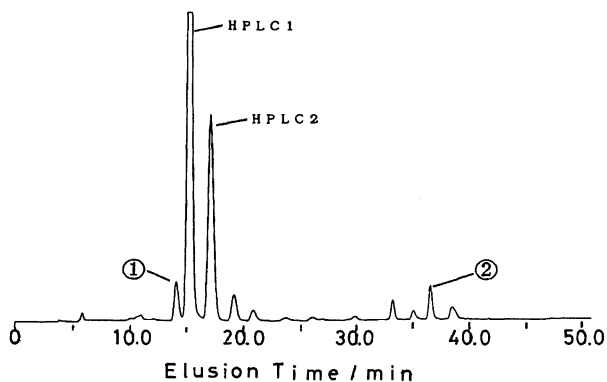


Fig. 1. HPLC elution profile of methanol extract of the *C. tepidum* cell. Elution solvent is methanol-water (96:4, v/v). Detection wavelength is 670 nm.

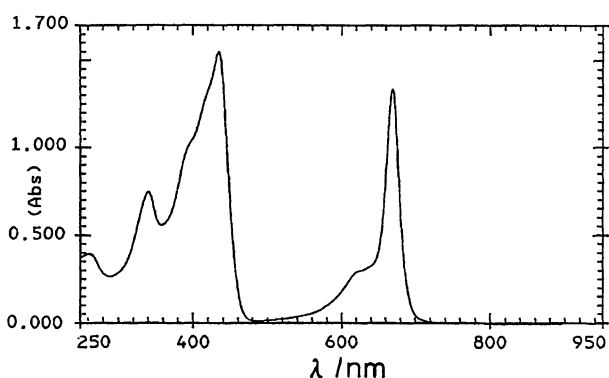


Fig. 2. Absorption spectrum for HPLC1 BChl c in methanol.

One dimensional and two dimensional (COSY)  $^1\text{H}$ NMR spectra were observed in  $\text{CD}_3\text{OD}$  for structural determination of HPLC1 and HPLC2 (data not shown). Homonuclear decoupling  $^1\text{H}$ NMR spectra were also observed (data not shown). The data demonstrate the presence of the basic BChl c conjugate structures in HPLC1 and HPLC2. Figure 3 illustrates the structures revealed from the  $^1\text{H}$ NMR assignments. Differences in structures among BChl c's from *Chloroflexus aurantiacus*,<sup>6)</sup> and *C. tepidum* were observed in the substituents at 4-, 5-, and 7-positions. The substituent at the 4-position in HPLC1 was determined as an ethyl group from the signals at 3.66 ppm (quartet) 4a- $\text{CH}_2$  and 1.60 ppm (triplet) 4b- $\text{CH}_3$ . While the substituent at the 4-position in HPLC2 was found to be a propyl group on the basis of the  $^1\text{H}$ NMR signals at 3.62 ppm (triplet) 4a- $\text{CH}_2$ , 2.08 ppm (sextet) 4b- $\text{CH}_2$ , and 1.15 ppm (triplet) 4c- $\text{CH}_3$ . The substituents at 5-position for both HPLC1 and HPLC2 were revealed to be ethyl groups from the signals at 3.92 (3.93) ppm (quartet) 5a- $\text{CH}_2$  and 1.77 (1.78) ppm (triplet) 5b- $\text{CH}_3$ . The candidates for the alkyl group of the alcohol which esterified with the propionic acid at the 7-position are farnesyl, phytanyl, and octadecyl. Only a farnesyl group gives the  $^1\text{H}$ NMR signals which are consistent with the observed

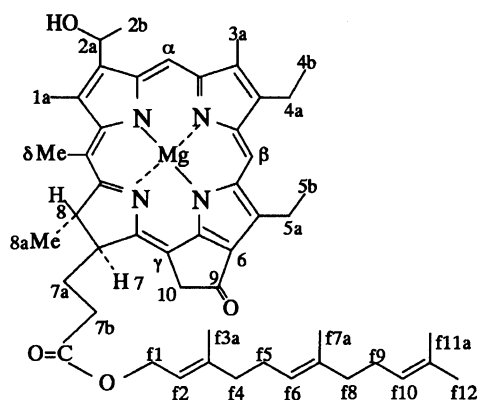
signals.

$^1\text{H}$ NMR spectra were obtained for HPLC1 in  $\text{CDCl}_3$ , and in  $\text{CDCl}_3$  with a small amount of  $\text{CD}_3\text{OD}$  (Fig. 4). Homonuclear correlated two dimensional  $^1\text{H}$ NMR (COSY) spectrum was also observed (data not shown) to aid the signal assignment. The  $^1\text{H}$ NMR resonances were assigned on the basis of these information together with a previous data in a literature for a similar dimer made of BChl d.<sup>15)</sup> It is revealed from Fig. 4, and a number of COSY peaks (data not shown) that in  $\text{CDCl}_3$  there exist a pair of resonances with an equal intensity for respective protons of HPLC1. This is apparent especially for  $\alpha\text{-H}$ ,  $\beta\text{-H}$ ,  $\delta\text{-CH}_3$ , 2b- $\text{CH}_3$ , and 3a- $\text{CH}_3$  protons. These facts indicate that BChl c exists in two different environments in  $\text{CDCl}_3$ . Since for BChl c aggregates, 5 coordination of the  $\text{Mg}^{2+}$  ion with the 2a-hydroxyl group has been established from the evidence of resonance Raman spectra<sup>16)</sup> and model experiments,<sup>17)</sup> we need to presume the presence of an asymmetric dimer model (a) or (d), or of the mixtures of two symmetric dimer models (b) and (c) in Fig. 5 to explain the  $^1\text{H}$ NMR data. The models (a) to (c) are head to head models where both 2a-hydroxyl groups coordinate to the magnesium ion of the other molecule. The model (a) is a piggy-back type, and the models (b) and (c) are a face to face type and a back to back type, respectively. The model (d) is a parallel head-to-tail model where the 2a-hydroxyl group of one molecule coordinates to the other molecule, and the 9-carbonyl group of one molecule coordinates to the other molecule. It should be noted that protons from 2b- $\text{CH}_3$  and  $\alpha\text{-H}$  show high field shifts. Since a ring current makes protons out of the ring plane shift to the high field, and makes ones in the plane shift to the low field, the observed results indicate that the 1-hydroxyethyl group in the 2-position should be out of plane, thus should coordinate to the magnesium ion of the other BChl c. Since the model (d) does not satisfy this qualitative consideration, we only need to consider the models (a) to (c). HPLC2 also gave similar  $^1\text{H}$ NMR spectra, thus indicating that the two major BChl c components form similar dimeric structures irrespective of the substituents at the 4-position.

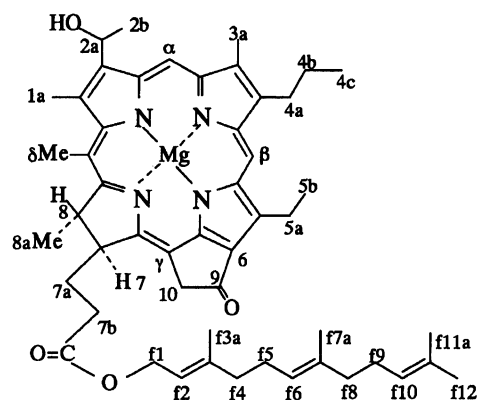
From Figs. 4a and 4b the chemical shift changes due to dimer formation were evaluated as the differences of the chemical shifts in  $\text{CDCl}_3$  from those in  $\text{CDCl}_3$  with a small amount of  $\text{CD}_3\text{OD}$ , where BChl c exists as a monomer. The results obtained were summarized in Table 1 together with calculated ring current shift data described below.

A ring current shift for a specific proton at a point R ( $\delta_R$ ) from surrounding monomeric unit was calculated by Abraham's double-dipole (ring current) model using the following equation,

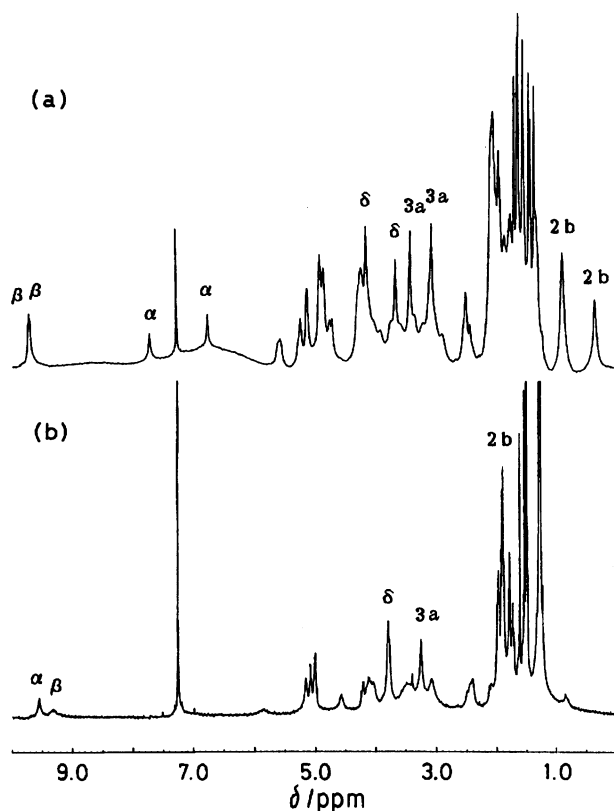
$$\delta_R = \sum_{i=1}^6 \frac{\mu_P}{\gamma_{iR}^3} (1 - 3 \cos^2 \theta_{iR}) + \sum_{j=1}^8 \frac{\mu_H}{\gamma_{jR}^3} (1 - 3 \cos^2 \theta_{jR}).$$



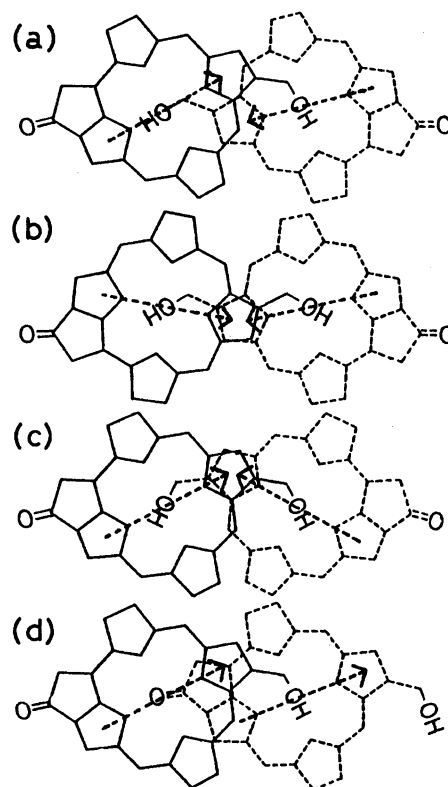
(1) HPLC1



(2) HPLC2

Fig. 3. Structures for HPLC1 and HPLC2 BChl c from *Chlorobium tepidum*.Fig. 4.  $^1\text{H}$  NMR spectrum of the HPLC1 in  $\text{CDCl}_3$  (a) and in  $\text{CDCl}_3$  with a small amount of  $\text{CD}_3\text{OD}$  (b).

Where  $\mu_P$  and  $\mu_H$  are the equivalent dipoles in the pyrrole ring and in the hexagon. The  $\gamma_{iR}$  and  $\theta_{iR}$  are the distance between the point R and the dipole, and the angle that  $\gamma_{iR}$  makes with the  $z$  axis.<sup>18,19</sup> Two kinds of equivalent dipoles,  $\mu_P$  and  $\mu_H$  were taken to be 19.0 and 22.0 Å<sup>3</sup>, respectively. Structural information was adopted from a literature of X-ray crystal data for BChl a.<sup>20</sup> The calculated results were summarized in Table 1 and compared with the experimentally observed chemical shift changes due to dimer formation. Since exper-

Fig. 5. Possible BChl c dimer models, (a) a head to head model (a piggy back type), (b) a head to head model (a face to face type), (c) a head to head model (a back to back type), and (d) a parallel head to tail model. The direction of  $Q_y$  band is depicted in the figures.

imentally a pair of signals were observed for respective protons, and either one of the symmetric models does not give a pair of the proton signals, and furthermore the chance to form either one of the symmetric dimers may be equal, we should compare the calculation values with the equal mixture of the symmetric dimers.

Thus for the symmetric dimers the calculation values should be combined and compared with the experimental ones. After considering these facts, we can propose from Table 1 that the model (a) offers the values which agree most with experimental values especially for  $\alpha$ -H,  $\delta$ -CH<sub>3</sub>, and 3a-CH<sub>3</sub> positions, where the ring current shift of these positions should be very sensitive to the aggregation structures of the models. The present calculation method may not be good for the protons where the distance from the ring is too short, because of the dipole approximation. This may explain the larger values calculated for 2a-CH as compared to the experimental ones.

Figure 6 shows absorption spectra of BChl c with variation in its concentrations. BChl c aggregates showed the Q<sub>y</sub> transitions centered around 677, 705, and 740 nm. Shorter wavelength components were predominant in lower concentrations of BChl c. Thus, with increase of BChl c concentrations, the components with 677, 705, and 740 nm peaks predominated in this order. This implies that higher and more stable aggregates formed with increase of BChl c concentrations, and that aggregates with absorption peaks at 677, 705 and 740 nm are formed stepwisely.

Figure 7a shows absorption spectra showing addition effects of dichloromethane on the BChl c aggregates in hexane-dichloromethane. Addition of dichloromethane gave pseudoisobestic points at 720 nm, indicating that the higher aggregate with absorption peak around 740 nm degraded to the lower aggregates with absorption peaks at 677 and 705 nm. Addition of methanol on the BChl c aggregates in hexane-dichloromethane solvent gave pseudoisobestic points at 700 nm indicating concomitant decrease of the 677 and 705 nm peaks with that of the 740 nm peak, and made increase of the BChl c monomer band at 663 nm (Fig. 7b). These results on solvent addition effects indicate that dichloromethane disrupts the 740 nm aggregate selectively without affecting the 677 and 705 nm aggregates, but that methanol degrades all the aggregates with absorption peaks at 677, 705, and 740 nm to the monomer with a 663 nm peak. Observed pseudoisobestic points represent changes between these two states, respectively.

We analyzed the origins for the stepwise spectral changes with a exciton theory<sup>21)</sup> by adopting a linearly oriented BChl c aggregate model. The exciton band energies were calculated by diagonalizing the following wave equation within the lowest excitation forming the Q<sub>y</sub> band of BChl c:<sup>22)</sup>

$$H\Psi_K = \varepsilon_K\Psi_K,$$

where  $\Psi_K$  is the  $K$ -th exciton wave function described by the next equation with a constant  $C_{Ki}$  and the BChl c lowest excitation wave function,  $\psi_i$ :

$$\Psi_K = \sum_{i=1}^N C_{Ki}\psi_i.$$

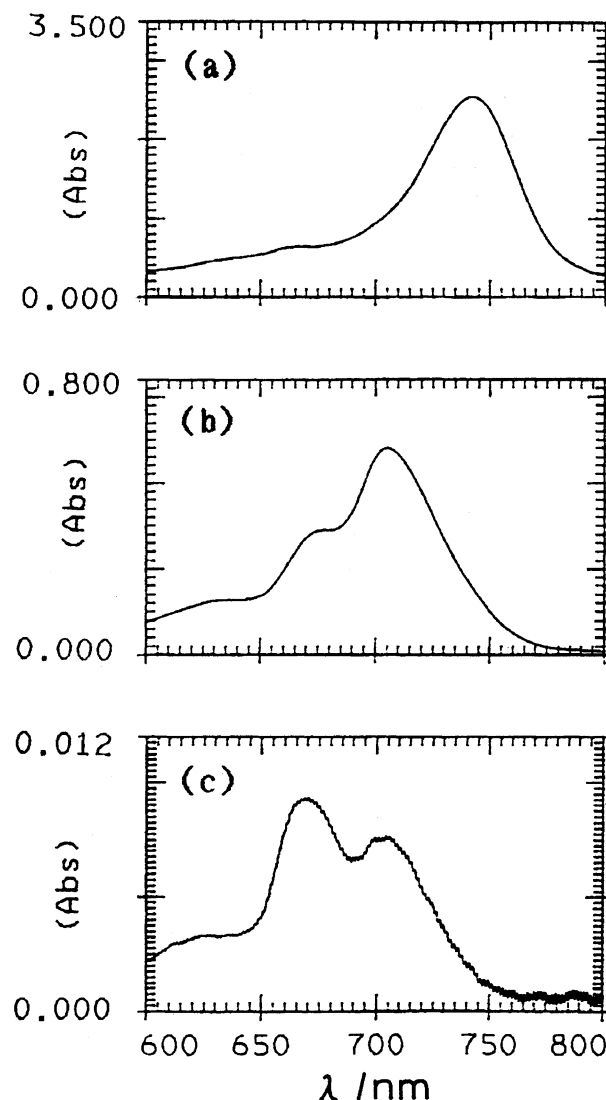


Fig. 6. Absorption spectrum for BChl c in various concentrations in hexane-dichloromethane (100:1, v/v). (a),  $6.0 \times 10^{-5}$  mol dm<sup>-3</sup>, in a 1 cm cell. (b),  $1.0 \times 10^{-5}$  mol dm<sup>-3</sup>, in 1 cm cell. (c),  $2.0 \times 10^{-7}$  mol dm<sup>-3</sup>, in 1 cm cell.

The hamiltonian  $H$  can be represented as

$$H = \sum_{i=1}^N |i\rangle E_i \langle i| + \sum_{i \neq j=1}^N |i\rangle V_{ij} \langle j|,$$

where the energy positions  $E_i$  are parameters which were taken as the monomeric BChl c transition energies for Q<sub>y</sub> bands ( $1.51 \times 10^4$  cm<sup>-1</sup> (662.5 nm)). The interaction energies  $V_{ij}$  were calculated with the dipole approximation by the following equation.

$$V_{ij} = 5.04 \frac{\gamma_{ij}^2 \mu_i \mu_j - 3(\gamma_{ij} \cdot \mu_i)(\gamma_{ij} \cdot \mu_j)}{\gamma_{ij}^5},$$

where  $\mu_n$  is the transition dipole moment of the  $n$ -th pigment and  $\gamma_{ij}$  is the vector connecting the centers of the pigments  $i$  and  $j$ . The absolute value of  $\mu_n$  was taken from the experimental value as  $\sqrt{30}$  D ( $D = 10^{-18}$  esu cm).<sup>11)</sup>

Table 1. Observed and Calculated Ring Current Shift Values

|                           | Observed<br>chemical shift<br>differences/ppm | Calculated ring current shift (ppm) |                |                |
|---------------------------|---|-------------------------------------|----------------|----------------|
|                           |   | (a) Asymmetric<br>(Piggy back)      | (b) Symmetric  |                |
|                           |   |                                     | (Face to Face) | (Back to Back) |
| $\alpha$ -H               | -1.85   | -2.09                               | -1.40          | -4.07          |
|                           | -2.83   | -3.38                               |                |                |
| $\beta$ -H                | 0.38  | 0.18                                | 0.17           | 0.20           |
|                           | 0.36  | 0.16                                |                |                |
| $\delta$ -CH <sub>3</sub> | 0.33  | 0.18                                | 0.03           | 0.12           |
|                           | -0.15   | -0.22                               |                |                |
| 2a-CH                     | -2.54   | -5.37                               | -5.55          | -4.63          |
|                           | -3.32   | -5.39                               |                |                |
| 2b-CH <sub>3</sub>        | -1.02   | -2.21                               | -2.41          | -2.17          |
|                           | -1.56   | -2.43                               |                |                |
| 3a-CH <sub>3</sub>        | 0.15  | 0.11                                | 0.09           | -1.23          |
|                           | -0.21   | -0.19                               |                |                |

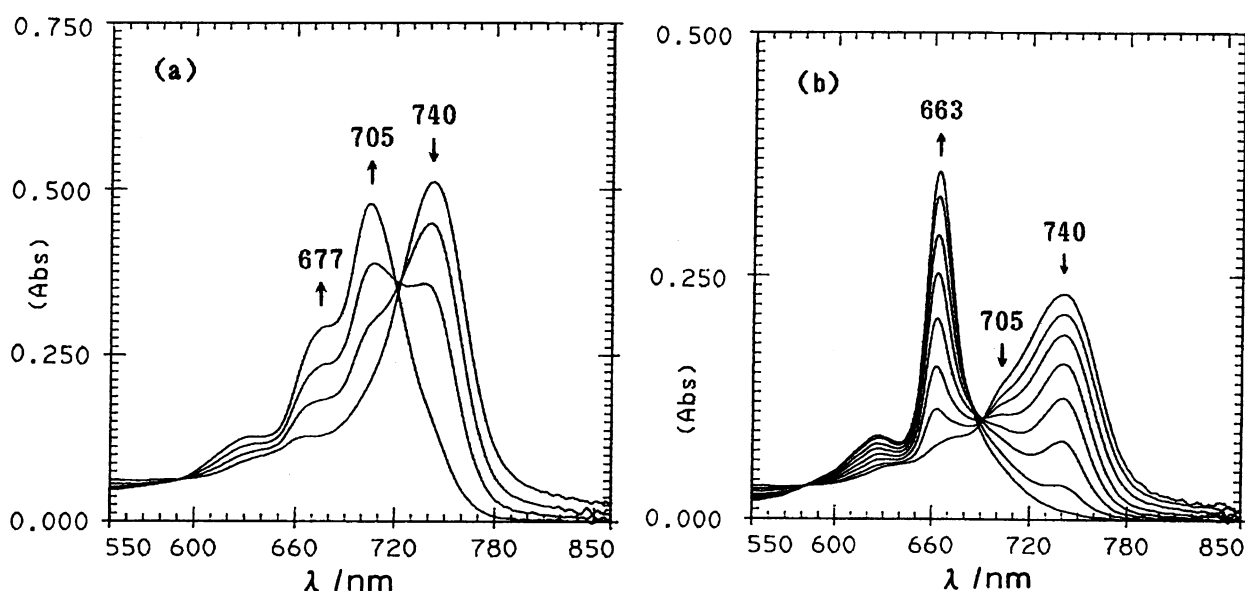


Fig. 7. Absorption spectra for BChl c  $6.0 \times 10^{-5}$  mol dm<sup>-3</sup> in hexane (1 ml) with various concentration of dichloromethane of 10, 30, 50, 70  $\mu$ l (a), and methanol of 0, 1, 2, 3, 4, 5, 6, 7  $\mu$ l (b).

The structures adopted were those extended from the piggy-back dimer established from the previous <sup>1</sup>H NMR experiments. The side-view can be drawn as that in Fig. 8 and the top-view is an extension of the structure in Fig. 5a. Parameters necessary for the calculation are easily estimated from the structure. For examples the angle between the dipoles in the neighboring BChl c's is calculated as 171° and the distance between the two BChl c dipoles in the dimer unit as 7.38 Å. The exciton theory tells that interactions between transition moments depend on their angles, and are inversely proportional to the cube of their distances. The theory, therefore, predicts significant red-shifts for dimer formation from monomers, and for tetramer formation<sup>23)</sup> from dimers. Actually model calculations showed a major red-shift both for dimer and tetramer formations, and minor red-shifts for the formations of aggre-

gate beyond tetramer (Table 2). Hence we attributed the observed first and second large stepwise spectral changes to the dimer and tetramer formations, respectively. The observed third stepwise absorption change needs, therefore, much higher ordered arrangements. This idea brought us to a "direct ring overlap" model among the linear BChl c aggregates (Fig. 8a) as shown in Fig. 8b. The direct ring overlap of this type makes feasible each BChl c ring closer than that within the linear aggregates where there exist a coordination bond of the 2a-hydroxyl group to the magnesium ion. The relative arrangement of the linear aggregates, i.e. the distance between the centers of two bacteriochlorophyll magnesium ions was selected as 3.9 Å which gave the longest wavelength shift. The value was found to be consistent with those of the ring current shifts estimated from cross polarization/magic angle spinning <sup>13</sup>C NMR

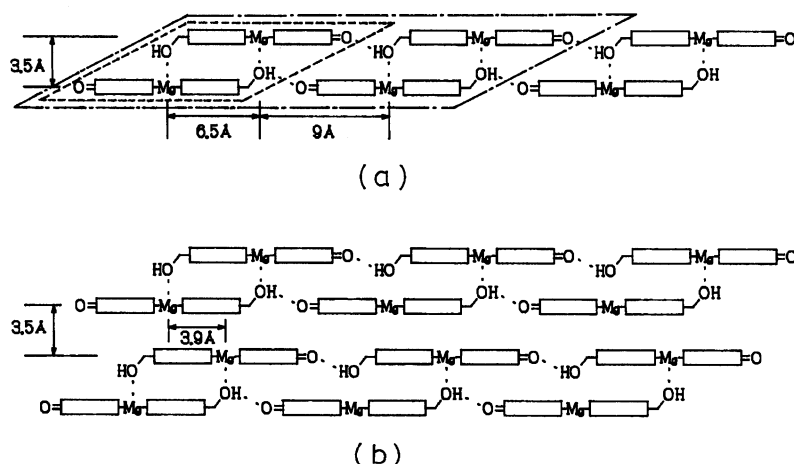


Fig. 8. Model bacteriochlorophyll c aggregate. A linear aggregate (a) and a direct ring overlap model (b). The dimer and the tetramer units are drawn within lines (---) and (-.-), respectively.

Table 2. Results of Exciton Theoretical Calculations for BChl c Aggregates

| Linear aggregate<br>(Fig. 8a) No. of<br>BChl c $\lambda$ /nm |       | Ring overlap model<br>(Fig. 8b) No. of<br>BChl c $\lambda$ /nm |       |
|--|-------|--|-------|
| 1  | 662.5 |  |       |
| 2  | 685.1 | 4  | 699.0 |
| 4  | 696.7 | 8  | 714.5 |
| 6  | 701.8 | 12   | 722.2 |
| 8  | 704.6 | 16   | 726.4 |
| 10   | 706.2 | 20   | 729.0 |
| 12   | 707.2 | 24   | 730.7 |
| 14   | 708.0 | 28   | 731.9 |
| 16   | 708.5 | 32   | 732.7 |
| 18   | 708.9 | 36   | 733.4 |
| 20   | 709.2 | 40   | 733.9 |
| 30   | 710.0 |  |       |
| 40   | 710.3 |  |       |

results.<sup>14)</sup> Actually exciton theoretical calculations on the higher ordered structures (Fig. 8b) among linear aggregates made of 20 BChl c's resulted in the red-shift to 733.9 nm (Table 2).

The presently proposed model, i.e. the direct ring overlap model, is reasonably consistent to the observed solvent effects on the BChl c aggregates described above. The high ordered arrangements of BChl c aggregates absorbed around 740 nm are stabilized by  $\pi$ -electron interactions, while the linear aggregates absorbed at 677 and 705 nm are stabilized by coordination bonds of the hydroxyl group to  $Mg^{2+}$  ion. The latter interactions should be very sensitive to a hydroxyl group, which can competitively coordinate to  $Mg^{2+}$  ion, while the former interactions should be sensitive to polar solvents even without coordination ability.

The close similarities of the absorption spectra and the solid state  $^{13}C$  NMR spectra<sup>14)</sup> between the model systems described here and the native chlorosomes im-

plies that they have similar BChl c aggregates. Moreover the environment of BChl c in chlorosomes can be presumed to be nonpolar as in BChl c aggregates in hexane. Considering the highly ordered arrangement of the linear aggregates, and the size of the rod-elements of 50 Å diameter in chlorosomes, we tentatively proposed the organization of BChl c's in the rod-elements in chlorosomes as shown in Fig. 9. This arrangement is consistent with the experimental results of linear dichroism which showed the direction of  $Q_y$  transition moments is almost parallel to the long axis of chlorosomes.<sup>24)</sup> The vertical arrangement of the ring to the periphery of the rod which makes feasible the direct ring overlap between the linear aggregate is unique in this model. The farnesyl tails at position 7 get together toward the inside of the rod in this model, however there is no direct experimental evidence for this arrangement. It may be possible that half of the tail forwards to the outside.

In conclusion it revealed that the thermophilic green sulfur bacterium *C. tepidum* have two major BChl c components with several minor BChl c frac-

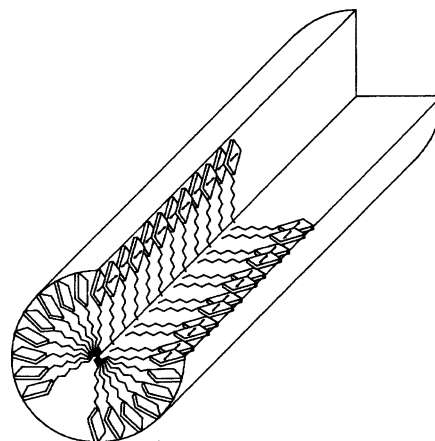


Fig. 9. Predicted organization of bacteriochlorophyll c's in chlorosomes.

tions.  $^1\text{H}$ NMR investigation disclosed that HPLC1 and HPLC2 have basic BChl c conjugate structures with a farnesol ester at the 7-position, and an ethyl group at the 5-position. At the 4-position HPLC1 possesses an ethyl group and HPLC2 has a propyl group. BChl c's form a piggy-back type dimers in  $\text{CDCl}_3$  irrespective of the substituent (either an ethyl or a propyl) at the 4-position. BChl c aggregates with absorption maxima around 677, 705, and 740 nm showed stepwise interchanges in hexane-dichloromethane with variations in BChl c concentrations and solvent compositions. Exciton theoretical analysis of the stepwise spectral shifts predicted high ordered organization of BChl c, implying a model for rod-elements in chlorosomes.

This work was supported by a Grant-in-Aid from the Ministry of Education, Science and Culture, and from Asahi Glass Foundation.

## References

- 1) T. M. Wahlund, C. R. Woese, R. W. Castenholz, and M. T. Madian, *Arch. Microbiol.*, **156**, 81 (1991).
- 2) J. M. Olson, *Biochim. Biophys. Acta*, **594**, 33 (1980).
- 3) L. A. Staehelin, J. R. Golecki, and G. Drews, *Biochim. Biophys. Acta*, **589**, 30 (1980).
- 4) A. R. Holzwarth, K. Griebenow, and K. Schaffner, *Z. Naturforsch., C*, **45**, 203 (1990).
- 5) W. Wullink, J. Knudsen, J. M. Olson, T. E. Redlinger, and E. F. J. van Brugger, *Biochim. Biophys. Acta*, **1060**, 97 (1991).
- 6) D. C. Brune, T. Nozawa, and R. E. Blankenship, *Biochemistry*, **26**, 8644 (1987).
- 7) D. C. Brune, P. D. Gerola, and J. M. Olson, *Photosynth. Res.*, **24**, 253 (1990).
- 8) J. M. Olson, D. C. Brune, and P. D. Gerola, "Molecular Biology of Membrane-Bound Complexes in Phototrophic Bacteria," ed by G. Drews and E. A. Dawes, Plenum Press, New York (1990), pp. 227—234.
- 9) M. L. Lutz and G. van Brakel, "Green Photosynthetic Bacteria," ed by J. M. Olson, Plenum Press, New York (1988), pp. 23—34.
- 10) Z. Festisova, L. Shibaeva, and M. Fok, *J. Theor. Biol.*, **140**, 167 (1989).
- 11) R. M. Pearlstein, "Photosynthesis: Energy Conversion by Plants and Bacteria," ed by Govindjee, Academic Press, New York (1982), Vol. 1, pp. 293—330.
- 12) J. M. Olson, P. D. Gerola, G. H. van Brakel, R. F. Meiburg, and H. Vasmel, "Antennas and Reaction Centers of Photosynthetic Bacteria," ed by M. E. Michel-Beyerle, Springer-Verlag, Berlin (1985), pp. 67—73.
- 13) T. Nozawa, K. Ohtomo, M. Suzuki, Y. Morishita, and M. T. Madigan, *Chem. Lett.*, **1991**, 1763.
- 14) T. Nozawa, M. Suzuki, K. Ohtomo, Y. Morishita, H. Konami, and M. T. Madigan, *Chem. Lett.*, **1991**, 1641.
- 15) K. M. Smith, L. A. Kehres, and J. Fajor, *J. Am. Chem. Soc.*, **105**, 1387 (1983).
- 16) T. Nozawa, T. Noguchi, and M. Tasumi, *J. Biochem.*, **108**, 737 (1990).
- 17) D. C. Brune, G. H. King, and R. E. Blankenship, "Proc. Conf. on Organization and Function of Photosynthetic Antennas," ed by H. Scheer and S. Schneider, Walter de Gruyter, Berlin (1988), pp. 141—151.
- 18) R. J. Abraham and K. M. Smith, *J. Am. Chem. Soc.*, **105**, 1674 (1983).
- 19) R. J. Abraham, S. C. M. Fell, and K. M. Smith, *Org. Magn. Reson.*, **9**, 367 (1977).
- 20) H. Chow, R. Serlin, and C. Strouse, *J. Am. Chem. Soc.*, **97**, 7230 (1975).
- 21) R. M. Pearlstein, "Chlorophylls," ed by H. Scheer, CRC Press, Boca Raton (1991), pp. 1047—1078.
- 22) The direction of  $Q_y$  band is along the line connecting the I and III pyrrole nitrogens as shown in Fig. 5.
- 23) Since dimer was predicted to be the first aggregate stepwisely formed, tetramer may form directly from dimers without formation of trimer. The dimer and tetramer units were shown in Fig. 8a.
- 24) K. Matsuura, M. Hirota, K. Shimada, and M. Mimuro, private communication.